A fabric dependent constitutive model for sand liquefaction

Ali Lashkari
Department of Civil Engineering –Islamic Azad University of Shiraz, Iran

ABSTRACT
As indicated by numerous researchers, the elastic response of each granular medium gradually becomes anisotropic when the mass of grains is subjected to shear stress. Herein, a simple anisotropic elasticity theory is proposed. Then, the constitutive equations of an existing bounding surface sand plasticity model are generalized to include the possibility of anisotropic elasticity. Finally, several comparisons and simulations are provided to show the importance of the proposed modification. It is shown that the application of anisotropic elasticity theory in advance constitutive sand models can explain the sudden loss of shear stress upon reverse loading.

RÉSUMÉ
Comme indiqué par de nombreux chercheurs, la réponse élastique de chaque milieu granulaire devient graduellement anisotrope quand la masse des grains est soumise à l'effort de cisaillement. Ci-dessus, on propose une théorie anisotrope simple d'élasticité. Puis, les équations constitutives d'un modèle extérieur de bondissement existant de plasticité de sable sont généralisées pour inclure la possibilité d'élasticité anisotrope. En conclusion, plusieurs comparaisons et simulations sont fournies pour montrer l'importance de la modification proposée. On lui montre que l'application des modèles constitutifs anisotropes de sable de théorie d'élasticité à l'avance peut expliquer la perte soudaine d'effort de cisaillement sur le chargement renversé.

1 INTRODUCTION

Granular soils usually exhibit significant anisotropy in their mechanical behaviour. Anisotropy is generally originated from two main sources: inherent anisotropy, and induced anisotropy (Wong and Arthur 1985). Inherent anisotropy forms due to the effect of gravity acting on a mass of grains during deposition and hardly changes up to large shear strains. Using distinct element method, it has been shown that direction of grains in granular assemblies remains relatively unchanged in large deformations (Cundall and Strack 1983). Thus, anisotropy of grains' direction can be taken as a major source of inherent anisotropy (e.g., Li and Dafalias 2002, Yang et al. 2005). On the other hand, normal vectors to contact planes between grains change direction and gradually rotate toward the direction of major principal effective stresses (e.g., Oda and Konishi 1974, Tobita and Nemat-Nasser 1982, Anandrajah and Kuganenthira 1995). In the other word, during shear, the number of contact planes increase along major principal stress and decreases along direction of minor principal stress. As a result, soil stiffness is highly weakened when loading is applied toward the opposite direction (e.g., Tobita and Nemat-Nasser 1982). In a series of undrained tests, Finn et al. (1970) have shown that small amplitude preshearing relatively improves soil stiffness due to densification effect; however, the mentioned improvement is overshadowed when shear stress is beyond a certain threshold known as phase transformation at which contraction turns into dilation. When soil state passes beyond the phase transformation and soil begins to dilate, the grains contact points can easily rearrange and soil fabric associated with contact planes evolves. Similar observations are made by Ishihara et al. (1975), Ishihara and Okada (1978), Nemat-Nasser and Tobita (1982), and De Gennaro et al. (2004).

In the experimental studies on sand liquefaction subjected to cyclic loading, it has been observed that dense and medium-dense samples of sand eventually form a butterfly shape stress path and when this type of behaviour is commenced, stress path experiences a very small amount of mean principal effective stress close to zero in each cycle (e.g., Vaid and Chern 1985, Arulmoli et al. 1992; Yoshimine and Hosono 2000). By applying conventional constitutive model to simulate this problem, it is observed that the predicted stress path tend to be stabilize much before that of experiments. Dafalias and Manzari (2004) studied this issue and attributed it to the neglecting the effects of fabric evolution in conventional sand constitutive models. To overcome this shortcoming, Dafalias and Manzari (2004) modified dilatancy by establishing a direct dependence of on an evolving second order fabric tensor. It is worth mentioning that other similar works can be found in the literature (e.g., Wan and Guo 2001, Papadimitriou et al. 2001). It has been shown that the above-mentioned procedures can accurately improve the models capability in simulation of liquefaction under cyclic loading.

The existing sand models usually considers the effect of both inherent and induced anisotropy by relating their constitutive elements regarding to the plastic part of behaviour to a second order fabric tensor (e.g., Wan and Guo 2001, Papadimitriou et al. 2001, Li and Dafalias et al. 2002, Dafalias and Manzari 2004, Lashkari and Latifi 2007, Anandarajah 2008). On the other hand, it has been experimentally shown that anisotropy can affect the elastic branch of behaviour too (e.g., Geaham and Houlsby 1983, Hoque and Tatsuoka 1998, De Gennaro et al. 2004). Besides, accounting for anisotropic elasticity

can significantly improve the predictions of localization in granular soils (e.g., Gajo et al. 2004).

Herein, an existing simple bounding surface plasticity model is modified to consider the possibility of anisotropic elasticity. Various comparisons are provided to show the importance of the proposed modification.

2 DEFINITION OF STRESS AND STRAIN SPACES

The model is formulated in conventional triaxial space in which σ_1 is the principal stress along vertical direction and $\sigma_2=\sigma_3$ are other principal stresses in horizontal plane. Similar assumptions can be made for strains. ε_1 is the principal strain along vertical direction and $\varepsilon_2=\varepsilon_3$ are other principal strains in horizontal plane. Based on the mentioned definitions, mean principal effective stress, p, and shear stress, q, are defined as:

$$p = \frac{\sigma_1 + 2\sigma_3}{3} \qquad [1]$$

$$q = \sigma_1 - \sigma_3 \qquad [2]$$

Similarly, volumetric strain, ε_v, and shear strain, ε_q, are defined as:

$$\varepsilon_v = \varepsilon_1 + 2\varepsilon_3 \qquad [3]$$

$$\varepsilon_q = \frac{2}{3}(\varepsilon_1 - \varepsilon_3) \qquad [4]$$

All stress components are effective. Compressive stresses are assumed positive and dilation is assumed negative.

3 EXPERIMENTAL EVIDENCES ON ANISOTROPIC ELASTICITY IN SAND

When the response of a continuum is purely elastic, the constitutive rule relating the rates of stress and strain tensors is:

$$\dot{\boldsymbol{\sigma}} = \mathbf{E}\,\dot{\boldsymbol{\varepsilon}}^e \qquad [5]$$

where $\boldsymbol{\sigma}$ and $\boldsymbol{\varepsilon}$ are stress and strain tensors, respectively. $\mathbf{E}$ is the forth ranked tensor defining proportionality.

The Green type of elasticity has been used in majority of sand plasticity models. In this type of elasticity, $\mathbf{E}$ is:

$$\mathbf{E} = (K - \frac{2}{3}G)\,\delta_{ij}\delta_{kl} + G\,(\delta_{ik}\delta_{jl} + \delta_{il}\delta_{jk}) \qquad [6]$$

where K and G are elastic bulk and shear moduli, respectively. Based on Richart et al. (1970), one has:

$$G = G_0 \frac{(2.973 - e)^2}{1 + e}\sqrt{\frac{p}{p_{ref}}} \qquad [7]$$

$$K = \frac{2}{3}G\frac{1+\nu}{1-2\nu} \qquad [8]$$

In Eq. (7), e is the current amount of void ratio. p_{ref} is a reference pressure that can be taken as atmospheric pressure (i.e., 101 kPa). ν is the poisson's ratio. G_0 and ν are depends on material type. δ_{ij} equals 1 when $i = j$, and 0 when $i \neq j$.

Considering Eqs. (1-4), the Green type of elasticity will be in the following form in the triaxial case:

$$\begin{bmatrix}\dot{p}\\ \dot{q}\end{bmatrix} = \begin{pmatrix}K & 0\\ 0 & 3G\end{pmatrix}\begin{bmatrix}\dot{\varepsilon}_v^e\\ \dot{\varepsilon}_q^e\end{bmatrix} \qquad [9]$$

Let us assume that as a constraint, volume change is not allowed (i.e., $\dot{\varepsilon}_v^e = 0$). As a result, Eq. (9) implies that $\dot{p} = 0$ and $\frac{\dot{q}}{\dot{p}} = \infty$. It is worth noting that as a basic assumption, in a Green type of elasticity, the medium is assumed isotropic and the results obtained above are direct consequences of the assumption of isotropy.

Koseki et al. (1998) studied the undrained elastic behaviour of sand in triaxial and torsional shear tests by applying very small amplitude unloading/reloading cycles of shear stress during undrained loading. It is logical to assume that the measured sand behaviour immediately after applying small amplitude reverse loading is purely elastic, because experimental data indicate that the generated strains upon the very small reverse loading are fully reversible (Koseki et al. 1998). The effective stress path of a medium-dense (e=0.712, Dr = 69%) sample of Toyoura sand in torsional shear apparatus is illustrated in Figure 1. Samples were prepared by pluviation of air dried sand. After that, they were undergone isotropic consolidation to p_{in} = 100 kPa. As shown in Figure 1, the sample was unloaded at τ = 39.6 kPa just before phase transformation took place. In the subsequent cycles of shear stress, the sample formed a butterfly shape stress path. Several small amplitude unloading/reloading cycles were applied on sample during the mentioned stress path described above. When p = 96.15 kPa, an unloading/reloading process was applied on sample in contractive regime of behaviour. This unloading/reloading process is zoomed in Figure 2(a). As seen, the slope of the tangent to unloading/reloading curve (namely $\dot{q}/\dot{p}$) is nearly vertical. This is in agreement with the consequence of Eq. (9) which implies that for the case of constant volume isotropic elasticity, mean principal effective stress must be constant. Interestingly, drastic deviation from the above-mentioned is observed when unloading/reloading is applied in dilative regime of behaviour.

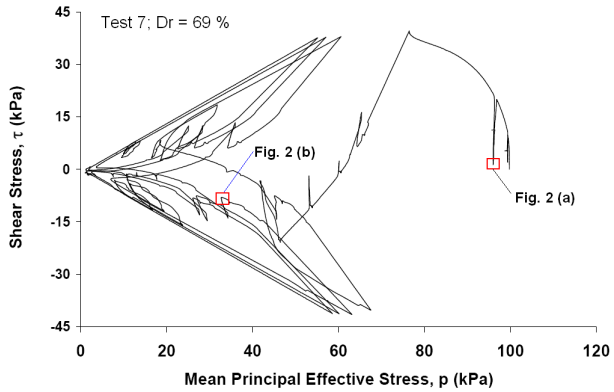

Figure 1. Effective stress path of a medium-dense sample of Toyoura sand subjected to undrained shear in torsional shear test (Koseki et al. 1998)

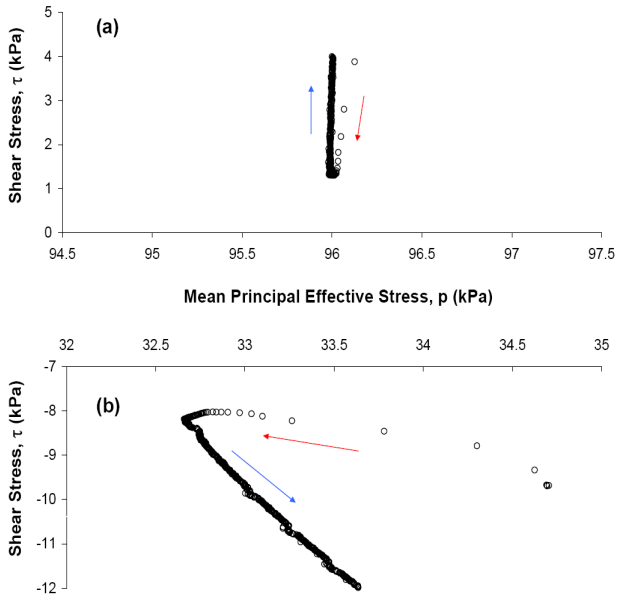

Figure 2. Effective stress path in zoomed parts of Figure 1 (after Koseki et al. 1998)

Using the same scale as Figure 2(a), an unloading/reloading process in dilative regime of behaviour shown in Figures 1 is zoomed in Figure 2(b). It can be seen that the slope of unloading curve in Figure 2(b) no longer remains vertical. This issue has been considered by many researchers as a seminal evidence of developed elasticity anisotropy (e.g., Graham and Houlsby 1983, De Gennaro et al. 2004).

4 DEVELOPMENT OF A SIMPLE ANISOTROPIC ELASTICITY THEORY

In the last section, experimental evidences are provided to show the link between soil general behaviour (either contractive or dilative) and evolution of anisotropic elasticity. In the literature of constitutive modeling, the elastic portion of behaviour has been usually assumed isotropic. The consequence of this issue on the prediction of advanced constitutive sand models will be further discussed in the part of model evaluation.

The second order fabric tensor is a versatile widely used concept that makes it possible to consider the effect of microstructure, fabric, of granular media into constitutive equations. A second order, traceless fabric tensor, **Z**, is introduced here as an index of microstructural evolution due to the history of the previous loadings. In the case of triaxial loading, **Z** can be defined as:

$$\mathbf{Z} = \begin{pmatrix} 2z & 0 & 0 \\ 0 & -z & 0 \\ 0 & 0 & -z \end{pmatrix} \qquad [10]$$

where z is an evolving scalar fabric variable. Similar to Dafalias and Manzari (2004), the following evolution rule is used for z:

$$\dot{z} = c_z \left\langle \dot{\varepsilon}_v^p \right\rangle (s\, z_{max} - z) \qquad [11]$$

where c_z is a material parameter and s is defined in the following section. Equation (11) varies z between z_{max} and $-z_{max}$ as the upper and lower boundaries of z. Finally, z_{max} is a model parameter. It is worth mentioning that z=0 when material is isotropic. Finally, s is a whole number that is defined in sequel.

Accounting only for the first order dependence and by using the representation theorem of isotropic functions (e.g., Tobita 1989, Ottosen and Ristinmaa 2005), the most general expression of **E** is:

$$\mathbf{E} = \phi_1\, \delta_{ij}\delta_{kl} + \phi_2\, (\delta_{ik}\delta_{jl} + \delta_{il}\delta_{jk}) + \phi_3\, (Z_{ij}\delta_{kl} + Z_{kl}\delta_{ij}) + \phi_4\, (Z_{ik}\delta_{jl} + Z_{il}\delta_{kj} + Z_{jk}\delta_{il} + Z_{jl}\delta_{ik}) \qquad [12]$$

where ϕ_i (i =1-4) are scalar functions of material type that must be determined experimentally with respect to physical considerations. Lashkari (2008) proposed the following configuration for ϕ_i (i =1-4):

$$\begin{aligned} \phi_1 &= (K - \frac{2}{3}G) \\ \phi_2 &= G \\ \phi_3 &= (K - \frac{2}{3}G) \\ \phi_4 &= 0 \end{aligned} \qquad [13]$$

Using Eqs. (5) and (12) together with Eqs. (1-4) yields the following relationship for the stress rates versus elastic strain rates with the possibility of anisotropic elasticity:

$$\begin{bmatrix} \dot{p} \\ \dot{q} \end{bmatrix} = \begin{pmatrix} K & (3K-2G)z \\ (3K-2G)z & 3G \end{pmatrix} \begin{bmatrix} \dot{\varepsilon}_v^e \\ \dot{\varepsilon}_q^e \end{bmatrix} = \begin{pmatrix} \Gamma_1 & \Gamma_2 \\ \Gamma_2 & \Gamma_3 \end{pmatrix} \begin{bmatrix} \dot{\varepsilon}_v^e \\ \dot{\varepsilon}_q^e \end{bmatrix} \qquad [14]$$

As seen, when material is anisotropic ($z \neq 0$), non-diagonal terms appears in the stiffness matrix and induce some cross-coupling effect between volumetric and shear strains. This can explain the behaviour shown in Figure 2 (b).

5 GENERAL FORMULATION OF A CRITICAL STATE BOUNDING SURFACE PLASTICITY MODEL

The critical state bounding surface plasticity model of Manzari and Dafalias (1997) is modified here to include the anisotropic elasticity introduced in the last section.

Volumetric and shear strain rates are decomposed into elastic and plastic parts as:

$$\begin{aligned} \dot{\varepsilon}_v &= \dot{\varepsilon}_v^e + \dot{\varepsilon}_v^p \\ \dot{\varepsilon}_q &= \dot{\varepsilon}_q^e + \dot{\varepsilon}_q^p \end{aligned} \qquad [15]$$

where superscripts “e” and “p” stand for elastic and plastic parts of strain rate, respectively.

A wedge region defines yield surface, domain of pure elasticity, in q-p plane (see Figure 3):

$$f = |\eta - \alpha| - m = 0 \qquad [16]$$

In above equation, f is yield surface, η = q / p is stress ratio, m is a parameter defining the yield surface size, and α is the angle that the wedge bisecting line makes with the positive direction of the p-axis due to kinematic hardening. Isotropic hardening, increase in the yield

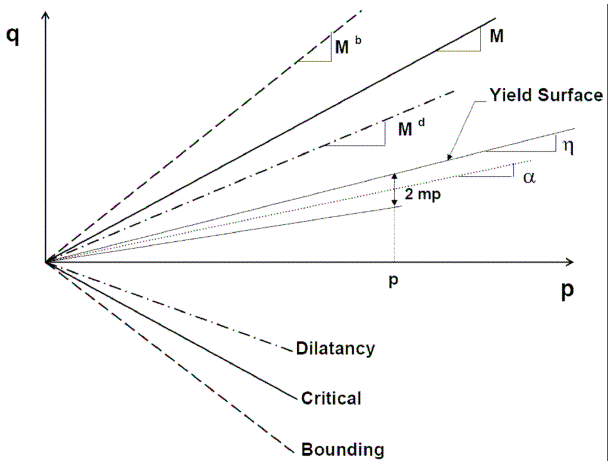

Figure 3. The model constitutive surfaces in triaxial stress space (Manzari and Dafalias 1997)

surface size, is omitted here. According to plasticity theory, plastic strains rate can be obtained from the following constitute equations when stress state attempts to move beyond the yield surface:

$$\dot{\varepsilon}_q^p = \frac{\dot{\eta}}{K_p} \qquad [17]$$
$$\dot{\varepsilon}_v^p = d\left|\dot{\varepsilon}_q^p\right|$$

In above equations, K_p is plastic modulus that is defined by:

$$K_p = h_0(1-c_h e)\frac{M^b - s\,\eta}{|\eta - \eta_{in}|}\sqrt{\frac{p_{ref}}{p}} \qquad [18]$$

Where h_0 and c_h are model parameter and η_{in} is the initial amount of η when the most recent loading starts. M^b indicated the bounding surface size as illustrated in Figure 3:

$$M^b = M\exp(-n^b\,\psi) \qquad [19]$$

M is the amount of stress ratio at critical state. M equals M_c when $\dot{q}$ is toward the positive direction of q-axis, and M_e otherwise. Both M_c and M_e are model parameters. ψ (= e - e_c) is the state parameter of Been and Jefferies (1985) in which e_c is the amount of void ratio on critical state line corresponding to the current amount of void ratio. According to Li and Wang (1998), the critical state line is defined by:

$$e_c = e_0 - \lambda\,(p/p_{ref})^{\xi} \qquad [20]$$

where e_0, λ, and ξ are model parameters. Finally, in Eq. (19), n^b is a model parameter.

Considering Figure (3) and in accordance to Dafalias and Manzari (2004), s takes +1 when η - α = m, and -1 when α - m =η.

In Eq. (17), d defines dilatancy:

$$d = A_d\,(M^d - s\,\eta) \qquad [21]$$

where

$$M^d = M\exp(n^d\,\psi) \qquad [22]$$

A_d and n_d are model parameters.

In triaxial space, plastic shear strain rate can be defined by:

$$\dot{\varepsilon}_q^p = \langle L \rangle\, s \qquad [23]$$

Now by considering the general definition of $\dot{p}$ and $\dot{q}$ given in Eqs. (14), one has:

$$\dot{p} = \Gamma_1\,\dot{\varepsilon}_v^e + \Gamma_2\,\dot{\varepsilon}_q^e = \Gamma_1\,(\dot{\varepsilon}_v - d\,L) + \Gamma_2\,(\dot{\varepsilon}_q - s\,L)$$
$$\dot{q} = \Gamma_2\,\dot{\varepsilon}_v^e + \Gamma_3\,\dot{\varepsilon}_q^e = \Gamma_2\,(\dot{\varepsilon}_v - d\,L) + \Gamma_3\,(\dot{\varepsilon}_q - s\,L) \qquad [24]$$

Implementing Eqs. (24) into Eq. (17-a) and rearrangement of some terms yield:

$$L = \frac{(\Gamma_3 - \eta\,\Gamma_2)\,\dot{\varepsilon}_q + (\Gamma_2 - \eta\,\Gamma_1)\,\dot{\varepsilon}_v}{s\,p\,K_p + s\,(\Gamma_3 - \eta\,\Gamma_2) + d\,(\Gamma_2 - \eta\,\Gamma_1)} \qquad [25]$$

6 THE MODEL EVALUATION

The model totally has 15 parameters. A systematic calibration procedure for these parameters is given in Manzari and Dafalias (1997), Dafalias and Manzari (2004), and Papadimitriou et al. (2001). The amounts of model parameters used in simulations are given in Table 1.

Figure 4 compares stress paths and shear stress

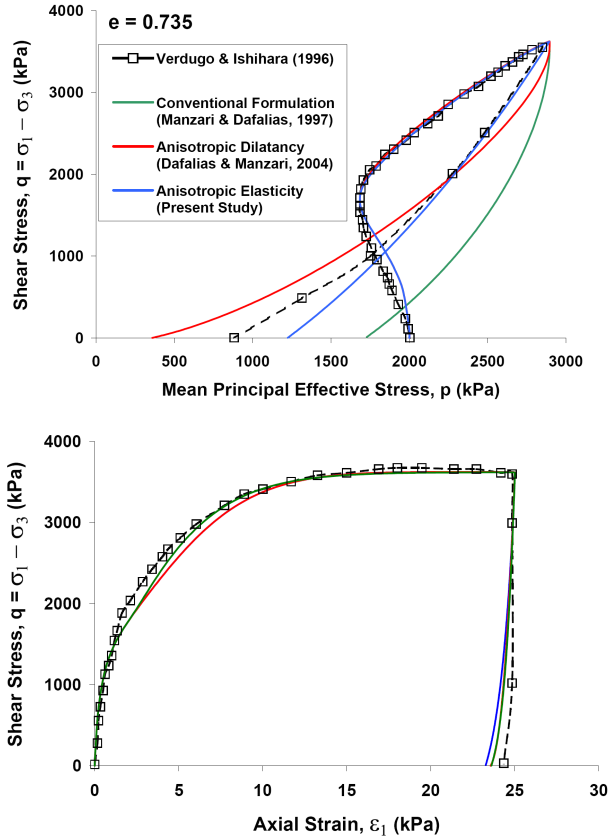

Figure 4. Comparisons of prediction obtained from various approaches with experimental results on an undrained loading/reverse loading test on a dense (e=0.733) sample of Toyoura sand (Data from Verdugo and Ishihara 1996)

versus axial strain curves obtained form the conventional plasticity theory which ignores fabric effect (e.g., Manzari and Dafalias 1997), the model of Dafalias and Manzari (2004) which considers anisotropy in definition of dilatancy, the model of this study with anisotropic elastic response, and experimental data on a dense (e=0.735) sample of Toyoura sand subjected to shear in triaxial apparatus. It is worth mentioning both model of this study and model of Dafalias and Manzari (2004) have been essentially built upon the framework of Manzari and Dafalias (1997). Thus, direct comparison of predictions is legitimate. As shown, all three approaches predict the same response upon loading. Considering unloading paths, the conventional model prediction is not realistic compared with experiment. Both model of this study and model of Dafalias and Manzari (2004) which account for the effect of fabric evolution are relatively capable to predict sudden loss of shear strength upon reverse loading. Besides, the model of this study underestimates the loss in mean principal effective stress when the sample is fully unloaded. On the other hand, it can be seen that the model of Dafalias and Manzari (2004) overestimates this effect.

Figure 5 illustrates comparison between predictions of the model of this study and their experimental counterparts. Tests are three medium-loose (e = 0.790 - 0.816) samples of Fuji river sand subjected to cyclic shear with different amplitudes in triaxial apparatus. The pattern of development of anisotropy and the model capability to duplicate this phenomenon can be examined in this figure. For example, please consider the part “a” of Figure 1. The sample only experience contraction, when it was unloaded in q=60 kpa. Hence, the amount of fabric evolution must be negligible and it is expected that the sample response upon unloading be isotropic and unloading path must be vertical with respect to p-axis.

Table 1. Amounts of model parameter in simulations.

Category	Parameter	Toyoura sand	Fuji River sand
Elastic	G_0	125.0	75.0
	ν	0.05	0.05
Yield surface	m	0.01	0.01
Critical state	M_c	1.25	1.45
	M_e	0.89	1.0875
	λ	0.019	0.0356
	e_0	0.934	0.90
	ξ	0.70	0.70
Plastic modulus	h_0	881.25	135.0
	c_h	0.968	0.0
	n^b	1.10	0.65
Dilatancy	A_0	0.704	0.75
	n^d	3.50	3.50
Fabric	z_{max}	3.0 ¶ 4.0 §	3.3
	c_z	1500.0 ¶ 600.0 §	1500.0

¶ : used in model of present study
§ : used in Dafalias and Manzari (2004)

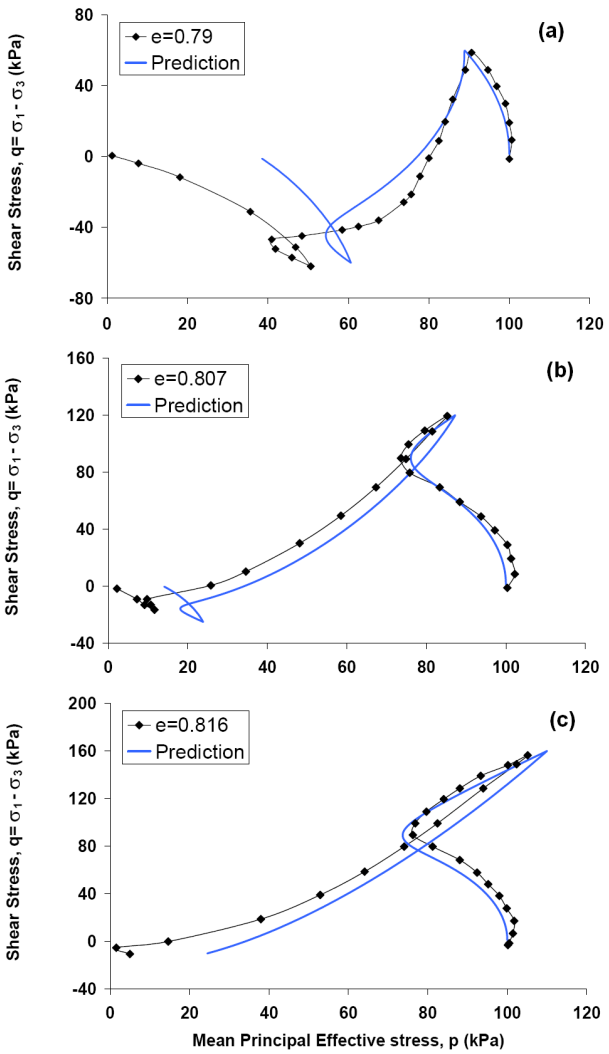

Figure 5. Simulations versus experiments in three undrained tests on three medium-loose samples of Fuji River sand (Data from Ishihara and Okada 1982)

As illustrated, the model prediction agrees with our expectation. Moreover, direction of loading once again was reversed when q reached -60 kPa. Unlike past, the sample was reloaded in dilative zone of behaviour. Thus, significant development of anisotropy within sample is expected. As seen, trace of the mentioned developed anisotropy is duplicated in the slope of reloading curve immediately after reloading. The same trends observed in parts “b” and “c” corroborates the assumed mechanism on emergence and development of anisotropy in elastic response of sand.

ACKNOWLEDGEMENTS

The Author would like to acknowledge Prof. J. Koseki for providing digital format of experimental data on Toyoura sand illustrated in Figures 1 and 2.

REFERENCES

Anandarajah, A. (2008). Multi-Mechanism anisotropic model for granular materials. *International Journal of Plasticity*, 24(5), 804- 845.

Anandarajah, A., and Kuganenthira, N. (1995). Some aspects of anisotropy of soil. *Géotechnique*, 45 (1), 69-81.

Arulmoli, K., Muraleetharan, K. K., Hossain, M. M., and Fruth, L. S. (1992). VELACS: verification of liquefaction analysis by centrifuge studies; laboratory testing program- soil data report. *Technical Report, the Earth Technology Corporation*, Irvine, California.

Been, K., and Jefferies, M. G. (1985). A state parameter for sands. *Géotechnique*, 35(2), 99-112.

Cundall, P.A. and Strack, O.D.L. (1983). Modeling of microscopic mechanisms in granular material. *Mechanics of Granular Materials: New Models and Constitutive Relations*, Jenkins, J.T. and Satake, M. eds., Elsevier, 137-149.

Dafalias, Y. F., and Manzari, M. T. (2004). Simple plasticity sand model accounting for fabric change effects. *ASCE Journal of Engineering Mechanics*, 130(6), 622-634.

De Gennaro, V., Canou, J., Dupla, J. C., and Benahmed, N. (2004). Influence of loading path on the undrained behavior of a medium loose sand. *Canadian Geotechnical Journal*, 41, 166-180.

Finn, W. D. L., Bransby, P. L., and Pickering, D. J. (1970). Effect of strain history on liquefaction of sand. *J. Soil Mech. Fdns. Div., ASCE* 96 (SM6), 1917- 1930.

Gajo, A., Bigoni, D., and Muir Wood, D. (2004). Multiple shear band development and related instabilities in granular materials. *Journal of Mechanics and Physics of solids*, 52, 2683-2724.

Graham, J. and Houlsby, G. T. (1983). Anisotropic elasticity of a natural clay. *Géotechnique*, 33(2), 165-180.

Hoque, E. and Tatsuoka, F. (1998). Anisotropy in elastic deformation of granular materials. *Soils and Foundations*, 38(1), 163-179.

Ishihara, K., Tatsuoka, F., and Yasuda, S. (1975). Undrained deformation and liquefaction of sand under cyclic stresses. *Soils and Foundations*, 15(1), 29-44.

Ishihara, K., and Okada, S. (1978). Effects of stress history on cyclic behavior of sand. *Soils and Foundations*, 18(4), 31-43.

Ishihara, K., and Okada, S. (1982). Effects of large preshearing on cyclic behavior of sand. *Soils and Foundations*, 22(3), 109-125.

Koseki, J., Kawakami, S., Nagayama, H., and Sato, T. (2000). Change of small strain quasi-elastic deformation properties during undrained cyclic torsional shear and triaxial tests of Toyoura sand. *Soils and Foundations*, 40(3), 101-110.

Lashkari, A., and Latifi, M. (2007). A simple plasticity model for prediction of non-coaxial flow of sand. *Mechanics Research Communications* 34(2), 191-200.

Lashkari, A. (2008). On the importance of accounting for anisotropic elasticity in granular soils. Under review for possible publication.

Li, X. S., and Wang, Y. (1998). Linear representation of steady state line for sands. *ASCE Journal of Geotechnical and Geoenvironmental Engineering*, 124(12), 1215-1217.

Li, X. S., and Dafalias Y. F. (2002). Constitutive modeling of inherently sand behavior. A*SCE Journal of Geotechnical and Geoenvironmental Engineering*, 128(10), 868-880.

Manzari, M. T., and Dafalias, Y. F. (1997). A critical state two-surface plasticity model for sands. *Géotechnique*, 47(2), 255-272.

Nemat-Nasser, S. and Tobita, Y. (1982). Influence of fabric on liquefaction and densification of cohesionless sand. Mechanics of Materials, 1, 43-62.

Oda, M., and Konishi, J. (1974). Microscopic deformation mechanism of granular material in simple shear. *Soils and Foundations*, 14(4), 25-38.

Ottosen, N. S., and Ristinmaa, M. (2005). *The mechanics of constitutive modeling*. Elsevier Publications, pp 1-700.

Papadimitriou, A. G., Bouckovalas, G. D., and Dafalias, Y. F. (2001). Plasticity modl for sand under small and large cyclic strains. *ASCE Journal of Geotechnical and Geoenvironmental Engineering*, 127(11), 973-983.

Richart, F. E. Jr., Hall, J. R., and Wood, R. D. (1970). *Vibration of soils and foundations*. Englewood Cliffs. NJ: Prentice Hall.

Tobita, Y. (1989). Fabric tensors in constitutive equations for granular materials. *Soils and Foundations*, 29(4), 99-104.

Vaid, Y. P., and Chern, J. C. (1985). Cyclic and monotonic undrained response of saturated sands. In; *Proceedings of, Advances in the Art of Testing Soils under Cyclic Loading*, ASCE, New York, 120-147.

Verdugo, R., and Ishihara, K. (1996). Steady state of sandy soils. *Soils and Foundations*, 36(2), 81-91.

Wan, R. G., and Guo, P. J. (2001). Effect of microstucture on undrained behavior of sand. *Canadian Geotechnical Journal*, 38, 16-28.

Wong, R. K. S., and Arthur, J. R. F. (1985). Induced and inherent anisotropy in sand. *Géotechnique*, 35(4), 471-481.

Yang, Z., Li, X.S., and Li, X. (2005) On relations between fabric anisotropy and mechanical behavior of granular soil. In: *Proceedings of McMat 2005: joint ASME/ASCE/SES Conference on Mechanics and Materials*, June 1-3, Baton Rouge, Louisiana, USA.

Yoshimine, M. and Hosono, Y. (2000). Effect of anisotropy of sand on results of undrained triaxial test. Memoir of graduate school of engineering. Tokyo Metropolitan University. 50, 158-169.